

# A Tabular Schedule Abstraction for Communication-Aware Evaluation of Pipeline-Parallel LLM Training

Daniel Barley\*, Jonathan Leis\*, Benjamin Klenk†, Holger Fröning\*

\* Hardware and Artificial Intelligence (HAWAII) Lab, Heidelberg University, Heidelberg, Germany

† NVIDIA Corporation, Santa Clara, CA, USA

{daniel.barley, holger.froening}@ziti.uni-heidelberg.de, jonathan.leis@stud.uni-heidelberg.de, bklenk@nvidia.com

**Abstract**—Pipeline parallelism is a key technique for distributed training of large language models because it reduces per-device parameter and activation memory. However, comparing pipeline schedules is difficult: analytical models expose structural quantities such as bubble ratios, while end-to-end hardware experiments are costly and system-specific. In this work, we introduce a tabular schedule abstraction and a unified multi-abstraction methodology that connects formula-based reasoning, idealized schedule tables, and communication-aware execution simulation.

Using this framework, we compare GPipe, 1F1B, Chimera, and Hanayo in its restricted regime across multiple modeled system configurations. Our results show that schedule rankings are not abstraction-invariant: communication can negate structural advantages suggested by bubble analysis alone. Under the assumptions considered here, GPipe and 1F1B are runtime-equivalent, but 1F1B achieves a lower activation-memory peak. Chimera is advantageous mainly at low microbatch counts and in communication-favorable regimes, while Hanayo is effective in its intended restricted operating point but remains sensitive to network bottlenecks. We further study an asymmetric Chimera-style placement, which does not reduce the global peak memory requirement but reveals limited runtime gains in shallow pipelines. Overall, pipeline schedule quality is meaningful only in the context of the modeled execution environment.

## I. INTRODUCTION

The training of large language models (LLMs) has emerged as a central large-scale distributed systems problem. As model size, sequence length, and training-token budgets continue to increase, single-device training is no longer feasible for practically relevant regimes [1], [2]. Contemporary training stacks therefore combine several forms of parallelism, most prominently data parallelism, tensor parallelism, and pipeline parallelism, in order to distribute both model state and computation across many accelerators [3]–[5].

While this distribution enables the training of models at unprecedented scale, it also fundamentally changes the performance bottlenecks that determine overall efficiency. Training throughput is no longer governed solely by local compute capability and memory bandwidth, but increasingly by inter-

device communication, synchronization, load imbalance, and schedule-induced idle time.

Within this design space, pipeline parallelism occupies a particularly important role because it reduces the per-device parameter and activation footprint by partitioning the model along network depth. However, the effectiveness of pipeline-parallel training depends not only on how layers are assigned to stages, but also on how forward and backward computations are scheduled across those stages [6]–[10]. Even for an identical partitioning of model parameters, different pipeline schedules can exhibit substantially different runtime and memory characteristics. These differences arise from variations in pipeline fill and drain behavior, activation retention time, communication exposure, and the degree to which communication can be overlapped with useful computation. As a result, pipeline scheduling should not be viewed merely as a theoretical question of bubble minimization, but as a systems problem shaped by the interaction of computation, memory, and communication under concrete execution constraints.

Despite its importance, the comparative evaluation of pipeline schedules remains methodologically challenging. Existing analyses often lie at one of two extremes. On the one hand, analytical or structurally idealized treatments can provide useful insight into quantities such as bubble ratios, memory peaks, or asymptotic utilization, but necessarily abstract away communication costs, cross-stage dependencies, and overlap effects. On the other hand, end-to-end experiments on large hardware installations provide realistic measurements, yet they are costly, difficult to control, and often tied to a particular system configuration, making systematic cross-regime comparison difficult. Between these extremes, simulation-based approaches provide an attractive middle ground by preserving explicit representations of computation, communication, and dependencies under configurable system assumptions [11], [12].

What is missing is a comparative workflow that connects these abstraction levels: one that preserves the interpretability of structural analysis while still incorporating the communication- and dependency-aware effects that ultimately shape distributed execution.

This work addresses that gap through a simulation-based study of synchronous pipeline schedules for distributed LLM

This work is part of the "Model-Based AI" project, which is funded by the Carl Zeiss Foundation. The authors acknowledge support by the state of Baden-Württemberg through bwHPC and the German Research Foundation (DFG) through grant INST 35/1597-1 FUGG.

training. Our work builds on Graphculon, a graph-based execution modeling and simulation framework for distributed LLM workloads, and extends it with a generalized schedule abstraction that represents pipeline schedules in a uniform tabular form. This abstraction separates schedule policy from execution-graph construction, simplifies the implementation of new schedules, and enables systematic extraction of structural metrics such as idle slots, fill/drain behavior, and activation lifetimes. In addition, it provides the basis for translating schedule descriptions into communication-aware execution graphs that can be simulated under configurable system assumptions. This enables a controlled comparison between three complementary views of a schedule: formula-based reasoning, idealized schedule tables, and runtime-oriented execution simulation.

Using this extended framework, we compare representative synchronous pipeline schedules, including GPipe [6], 1F1B [7], [8], Chimera [9], and Hanayo [10] (in its restricted regime), across multiple system regimes. Our results show that schedule rankings are generally not abstraction-invariant: conclusions drawn from formulas or idealized schedule tables do not necessarily carry over once communication and dependency structure are modeled explicitly. Under the assumptions considered in this work, GPipe and 1F1B are runtime-equivalent, but 1F1B achieves a lower peak memory footprint. Chimera can outperform unidirectional schedules, but primarily in regimes with small microbatch counts where its bidirectional execution can reduce structural idle time without being dominated by additional communication overhead. Hanayo is effective in its intended operating regime, yet remains sensitive to communication bottlenecks. These findings suggest that schedule quality should be interpreted as system-dependent rather than universal, and that structurally attractive schedules may lose their advantage when evaluated under more explicit execution models.

Beyond this comparative analysis, we also investigate a novel asymmetric Chimera-style placement in which model stages are distributed unevenly across the two counter-propagating branches. This case study is motivated by the hypothesis that asymmetric placement may alleviate memory pressure or improve runtime by reshaping where the critical path arises. The study indicates that asymmetric placements may yield limited runtime benefits in specific shallow-pipeline and communication-favorable regimes. However, our results do not support the anticipated memory advantage: the evaluated asymmetric 1:2 placement does not reduce the relevant per-device memory peak. This refines the design intuition around asymmetric schedules and illustrates the need for explicit bottleneck-aware evaluation.

Overall, this paper makes three contributions.

- First, we introduce a generalized tabular schedule abstraction for Graphculon that improves the expressiveness and comparability of pipeline schedule modeling.
- Second, we establish a unified multi-abstraction methodology for evaluating pipeline schedules, spanning

formulas, structural schedule representations, and communication-aware runtime simulation.

- Third, we use this methodology to derive comparative insights into established schedule families and to assess a novel asymmetric Chimera variant.

Taken together, our results argue for a more cautious and methodologically layered interpretation of pipeline schedule quality: efficient schedule design cannot be inferred reliably from structural formulas alone, but must be evaluated in the presence of communication, dependency, and memory interactions.

## II. BACKGROUND

Training large language models in distributed environments requires not only partitioning model state and computation across many devices, but also coordinating when intermediate results are produced, communicated, and consumed. In this context, pipeline parallelism is attractive because it reduces per-device model-state and activation requirements by partitioning the model along network depth and executing different microbatches concurrently across pipeline stages [4], [6]. However, its efficiency is governed not only by the stage partitioning itself, but also by the schedule that determines how forward and backward computations progress through the pipeline. This section briefly reviews the schedule families considered in this work and highlights why their comparison is not trivial.

### A. Pipeline-parallel training and scheduling

In pipeline-parallel training, a minibatch is divided into multiple microbatches that are injected into a sequence of pipeline stages. This enables different stages to process different microbatches concurrently, thereby improving device utilization compared to purely sequential execution [6]. The schedule determines in which order microbatches and their associated forward and backward phases are executed on each stage, and it therefore directly affects runtime, idle time, and memory usage.

The baseline is *GPipe* [6], which follows a fill-drain strategy: forward passes are first injected until the pipeline is full, and backward computation starts only after the full minibatch has reached the last stage (Figure 1a). This schedule is simple and exposes a clear structural bubble, but it retains activations for many microbatches simultaneously and thus incurs high activation-memory pressure. A more memory-efficient alternative is *1F1B* (one-forward-one-backward, Figure 1b), introduced in PipeDream and later adapted to synchronous execution in PipeDream-Flush, where stages alternate between forward and backward work once steady state has been reached [7], [8]. This reduces activation-retention intervals while largely preserving the pipeline structure.

More recent schedules modify the flow of work more aggressively. *Chimera* (Figure 1c) uses two counter-propagating pipelines to reduce structural bubbles through bidirectional execution, at the cost of increased communication and duplicated parameters [9]. *Hanayo* introduces a wave-like synchronous

schedule (Figure 1d) that aims to improve utilization without requiring the same degree of parameter duplication [10]. These schedules illustrate that pipeline scheduling is not a one-dimensional optimization problem: reducing bubble ratio may require additional communication, different parameter placement, or longer dependency chains.

Two structural quantities are especially important in this context. The first is the *pipeline bubble*, i.e., the fraction of time during which workers are idle because the pipeline is still filling, draining, or blocked by dependencies. The second is *activation lifetime*, which determines how long forward activations must remain resident until the corresponding backward computation consumes them. Bubble behavior primarily affects utilization and runtime, whereas activation lifetime strongly affects peak memory consumption. Both are schedule-dependent and therefore central to any meaningful comparison of pipeline schedules.

At the same time, these structural quantities do not fully determine practical performance. A schedule with an attractive bubble ratio may still perform worse if it exposes more communication, if communication cannot be overlapped with useful computation, or if additional persistent memory terms dominate the activation savings. This motivates the distinction between *structural reasoning*, which studies schedules through formulas or idealized slot-based representations, and *communication-aware execution modeling*, which incorporates explicit compute, communication, and dependency effects under system assumptions.

### B. Difficulty of schedule comparison

The comparative evaluation of pipeline schedules is difficult because different evaluation methods expose different aspects of schedule behavior. Analytical models provide compact expressions for quantities such as bubble ratios, nominal utilization, or peak activation counts, and are therefore useful for developing structural intuition [6], [9]. However, they abstract away many effects that are central in distributed execution, including communication cost, overlap constraints, and dependency-induced serialization. As a result, analytically favorable schedules need not remain favorable once those effects are taken into account.

At the other extreme, end-to-end experiments on hardware provide realistic measurements, but they are costly to run, difficult to control, and often tied to a particular system and software stack [4], [9], [10]. This makes it difficult to isolate schedule-specific behavior from other confounding factors and limits systematic exploration across system regimes. Simulation-based approaches provide a useful middle ground by representing computation, communication, and dependencies explicitly while keeping the underlying system parameters configurable [11], [12].

The key challenge is therefore not simply to measure a schedule under one particular setup, but to determine whether its qualitative ranking remains stable across abstraction levels and system regimes.

## III. A MULTI-ABSTRACTION EVALUATION FRAMEWORK

This section introduces the schedule representation, its translation into an execution model, and the abstraction levels and metrics used in the subsequent evaluation.

### A. Tabular schedule abstraction

We represent a pipeline schedule as a discrete table over workers and time steps. Let  $W$  denote the number of workers and  $T$  the number of schedule slots. A schedule is defined as

$$S \in (\mathcal{M} \times \mathcal{P} \cup \{\emptyset\})^{W \times T},$$

where  $\mathcal{M}$  is the set of microbatches,  $\mathcal{P}$  the set of execution phases, and  $\emptyset$  denotes an idle slot. Thus, each entry  $S_{w,t}$  specifies that worker  $w$  executes phase  $p \in \mathcal{P}$  for microbatch  $m \in \mathcal{M}$  at slot  $t$ , or remains idle otherwise. In the setting considered here,  $\mathcal{P} = \{\text{fwd}, \text{agrad}, \text{wgrad}, \text{opt}, \text{recomp}\}$ , corresponding to forward computation, activation-gradient computation, weight-gradient computation, optimizer update, and optional activation recomputation.

This representation is intentionally structural rather than temporal. A table entry indicates that a phase is scheduled in a given slot, but does not yet assign a hardware-dependent duration to that slot. The abstraction therefore separates *schedule policy* from *execution cost*. This is useful for two reasons. First, it makes schedule properties such as idle slots, fill and drain behavior, and activation-retention intervals directly visible. Second, it allows different schedule families to share a common representation, while their communication and runtime implications are introduced only later through execution-graph construction and simulation.

Rows in the table correspond to *workers*, not necessarily to individual accelerators. A worker is treated as an abstract execution unit that may internally contain additional forms of parallelism, such as tensor or expert parallelism. The schedule abstraction therefore captures pipeline-level coordination without exposing worker-internal implementation details. A table is considered valid if each worker-time slot contains at most one phase, the causal ordering of phases for every microbatch is preserved, and all required phases are eventually scheduled. Overall, the tabular abstraction serves as a compact intermediate representation between abstract schedule design and communication-aware execution modeling. Example schedule tables are shown in Figure 1.

### B. From schedule tables to execution graphs

The tabular schedule abstraction defines what is executed on each worker and in which discrete slot, but it does not yet encode the explicit dependency structure required for communication-aware simulation. To obtain such a representation, each schedule table is translated into an execution graph whose nodes represent compute and communication events and whose edges capture the causal dependencies between them.

The translation proceeds in two steps. First, the table is traversed row-wise to derive the *worker-local execution order*. Each non-empty cell is mapped to the corresponding compute



properties that are difficult to recover from formulas alone. At the same time, this level remains intentionally hardware-agnostic: all slots are interpreted structurally rather than as physical time.

The third and most detailed level is *communication-aware execution simulation*. Here, the schedule table is translated into an execution graph and annotated under a chosen compute and communication model. This makes it possible to capture system-dependent effects such as exposed communication, limited overlap between compute and communication, and the impact of different system regimes on runtime and memory behavior. While this level remains a model rather than a hardware-calibrated predictor, it provides a substantially more realistic basis for comparing schedules than structural reasoning alone.

Graphculon is a graph based analytical model based on Calculon [13] that allows us to implement the third level of evaluation. Graphculon uses the annotated compute graph to generate a timeline, as shown in Figure 2, using a capacity-based system model. Since the byte volume  $V_{\text{net}}$  of the communication is known from the graph, communication time  $t_{\text{comm}}$  can be calculated following the Hockney model:

$$t_{\text{comm}} = \frac{V_{\text{net}}}{\text{BW}_{\text{net}}} + L_{\text{net}}, \quad (1)$$

using the bandwidth  $\text{BW}_{\text{net}}$  and the latency  $L_{\text{net}}$ .

The compute time  $t_{\text{comp}}$  is obtained using a roofline based model

$$t_{\text{comp}} = \max\left(\frac{F}{\text{TP} \cdot e_c} + L_c, \frac{V_m}{\text{BW}_m \cdot e_m} + L_m\right), \quad (2)$$

where a memory-bound workload will be approximated based on the memory time defined by the byte volume  $V_m$ , memory bandwidth  $\text{BW}_m$  and latency  $L_m$  and for a compute-bound workload we swap bandwidth for peak throughput  $\text{TP}$  and the byte volume for the number of FLOPs  $F$  and add a startup latency of  $L_c$ . Two empirical efficiency terms model additional hardware effects.  $e_c$  estimates the percentage of achieved compute performance of the peak throughput based on the number of FLOPs, as does  $e_m$  for the memory based on the byte volume.

Using these three levels side by side serves two purposes. First, it allows us to separate *structure-driven* conclusions from *system-driven* conclusions. Second, it enables us to test whether schedule rankings are stable across abstraction levels or whether they change once communication and dependencies are modeled explicitly. This multi-abstraction perspective forms the methodological basis of our evaluation.

#### D. Metrics

Our evaluation focuses on two classes of metrics: *utilization- and runtime-related metrics* and *memory-related metrics*. Together, these capture the main trade-off space of synchronous pipeline schedules.

The first class characterizes how effectively a schedule keeps pipeline workers busy. At the formula and schedule-table levels, this is expressed through structural quantities such as

*bubble ratio*, *worker utilization*, and *schedule length in slots*. These metrics capture the amount of idle time induced by pipeline fill, steady-state execution, and drain, and therefore provide a hardware-agnostic view of how efficiently a schedule uses the pipeline. At the simulation level, the corresponding metric is the *modeled execution time* of one training step, which incorporates explicit compute, communication, and dependency effects under a chosen system model.

The second class captures *per-device memory pressure*. Here, the most important quantity is the *peak memory requirement* on the bottleneck worker. We distinguish in particular between *activation memory*, which is strongly schedule-dependent through activation-retention intervals, and persistent memory terms such as parameters, gradients, and optimizer state. This distinction is important because some schedules, such as bidirectional variants with parameter duplication, may reduce activation pressure while increasing persistent memory requirements. Accordingly, we consider both schedule-specific activation peaks and the resulting overall per-device memory footprint.

These metrics are compared across abstraction levels. Bubble ratios and slot-based schedule lengths capture structural properties of a schedule, whereas simulated execution time captures system-dependent behavior. Likewise, activation-retention patterns are visible already at the table level, but their practical impact must be interpreted together with the full memory composition of the worker. Our goal is therefore not to collapse all levels into a single scalar score, but to analyze which conclusions remain stable across levels and which emerge only once communication-aware execution is modeled explicitly.

## IV. EXPERIMENTAL SETUP

In our studies we analyze a Megatron [3] style model with 128 transformer blocks, a hidden dimension  $d_{\text{hidden}} = 4096$ , a number of attention heads  $n_{\text{heads}} = 80$ , sequence length  $s = 4096$ , and GELU [14] nonlinearity. We further assume a fixed global minibatch size. Changes to the number of microbatches  $B$  therefore change the computational work per microbatch. This study focuses on pipeline parallelism exclusively. The number of stages is denoted  $S$ . We do not vary data, tensor, or expert parallelism and set these domains to 1.

#### A. Schedules under study

In our experiments we evaluate GPipe, 1F1B, Chimera, and Hanayo, as described in Section II-A. The Hanayo schedule is specifically designed for  $S = B$  configuration and therefore excluded from the more exhaustive microbatch sweeps performed for the other schedules.

#### B. Modeled systems and regimes

To demonstrate system effects we model a 3 by 3 grid of configurations. This baseline system configuration models an NVIDIA DGX H100 compute node with roughly 1 PFLOPs of compute,  $34 \text{ TB s}^{-1}$  total memory bandwidth with a memory latency of 50 ns, and a  $50 \text{ GB s}^{-1}$  Infiniband interconnect

with a latency of 500ns. We then scale both the compute and network components by a factor of 10 in both directions to obtain a fast and slow compute system, `fast_cp` and `slow_cp` respectively, and fast and slow network system, `fast_nw` and `slow_nw`. Both throughput/bandwidth and latency are scaled.

Although this  $10\times$  scaling is stylized, it is not intended to be purely hypothetical: modern rack-scale scale-up fabrics such as NVIDIA NVL72 expose aggregate communication bandwidth far beyond conventional inter-node InfiniBand. We therefore interpret the fast-network regime as a communication-favorable envelope rather than as a direct model of a specific link technology.

### C. Scope and assumptions

Our study is of a comparative nature. Rather than predicting exact numbers for an explicit hardware target we want to explore the effects hardware has on communication schedules otherwise hidden at higher levels of abstraction. Additionally, we limit the scope to synchronous schedules with identical training semantics. Otherwise, comparisons would not be meaningful without also reporting convergence and accuracy metrics, requiring an actual training run which is out of the scope of this work.

## V. COMPARING PIPELINE SCHEDULES ACROSS ABSTRACTION LEVELS

This section compares the schedules listed in Section IV under the levels of abstraction listed in Section III. We first compare the analytical formulae to the time slot table view and move to communication-aware simulation afterward.

### A. Structural comparison without simulation

Comparing the closed-form formulae to the instantiated time slot table, as shown in Figure 3, already reveals some discrepancies for the Chimera schedule. GPipe and 1F1B not only behave the same in the analytical model, which is expected of course, but also match the tabular representation perfectly. Note that they overlap perfectly in the figure. For Chimera, however, we observe slightly larger bubble ratios using the tabular abstraction than we obtain from the formula. The effect is more pronounced for a smaller number of microbatches but still holds true for  $B = 256$ , albeit at a significantly smaller difference. We observe the same effect when varying the number of stages. At  $(S, B) = (8, 16)$  we obtain bubble ratios of 16% vs. 26% from formula and table respectively. At  $(S, B) = (4, 16)$  we similarly observe values of 6% vs. 13%.

Because we use the same timing assumptions ( $t_{\text{bwd}} = 2t_{\text{fwd}}$ ) in both cases and preserve the same bidirectional execution pattern from the original paper we conclude that the two abstraction levels disagree for Chimera. However, in all cases Chimera outperforms GPipe and 1F1B with a lower bubble ratio.

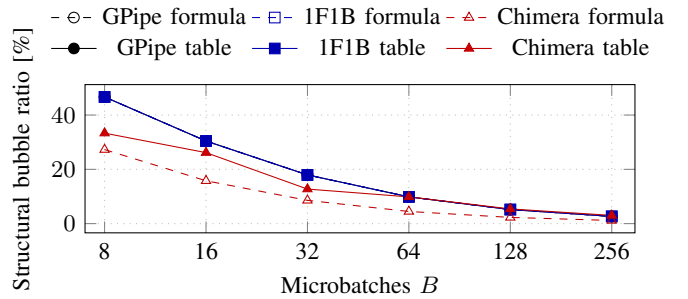


Fig. 3: Structural bubble ratio comparison between analytical formulae and time slot table abstraction for GPipe, 1F1B, and Chimera at number of pipeline stages  $S = 8$ . As expected, GPipe and 1F1B are equivalent in bubble ratio. This also translates directly to the tabular abstraction. For Chimera we observe the analytical formula to be more optimistic than the instantiated table.

### B. Runtime under communication-aware modeling

When we introduce explicit communication through simulation via Graphculon we immediately observe how side effects can alter the results. While Chimera consistently shows a lower or at least equal bubble ratio using the tabular abstraction, we observe, especially for network-bound systems, that GPipe and 1F1B offer a better idle to compute time ratio and overall runtime at a higher microbatch count. Simulating systems from network-bound to compute-bound confirms our thesis that the quality of schedule highly depends on the system configuration and training hyperparameters used, as we will elaborate in the following.

Figure 4 shows both simulated runtime and idle time for processing a minibatch and over 8 pipeline stages and various numbers of microbatches on three different systems. On network-bound systems we see that increasing the number of microbatches will even lead to longer runtimes. This intuitively makes sense as this leads to more communication overall. The more communication-heavy Chimera schedule is more affected by this than GPipe and 1F1B. On the baseline system the difference is less pronounced, but beyond 32 microbatches GPipe and 1F1B show better idle and runtime on a system. Finally, on a system with a very fast network compared to compute Chimera outperforms GPipe and 1F1B until a microbatch count of 64. Beyond that, the schedules converge.

### C. Memory behavior across schedules

One important factor not mentioned so far is the per-node peak memory required for the schedule in question. Even with recent development in datacenter-grade GPUs they are notoriously short on memory. In most cases peak memory consumption will dictate whether a schedule is feasible or not. We have already observed the structural and runtime differences among the schedules. They behave equally different in the memory domain.

Figure 5 shows the peak per-device memory for different microbatch counts and 4 and 8 pipeline stages. GPipe’s

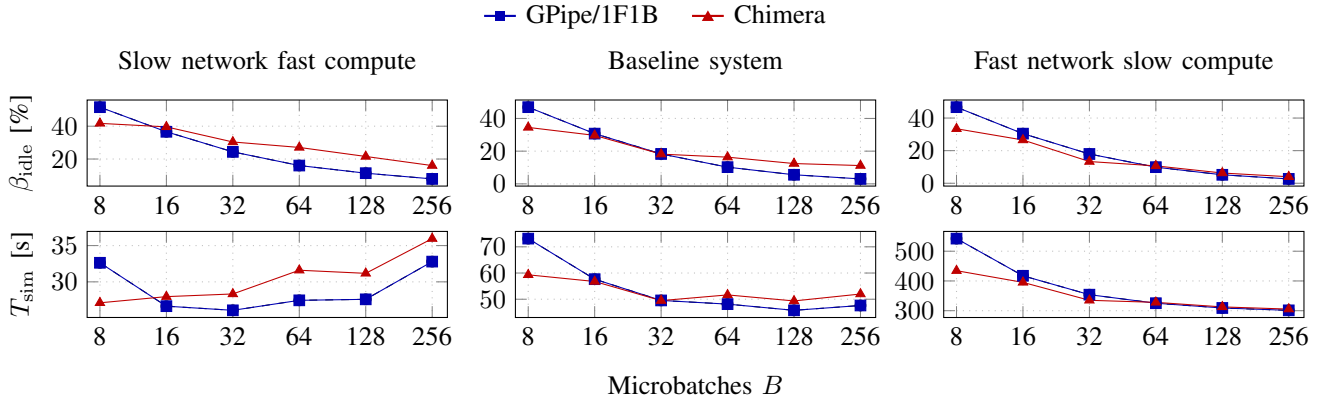


Fig. 4: Simulated runtime  $T_{sim}$  and idle time ratio  $\beta_{idle}$  comparison of GPipe, 1F1B, and Chimera processing a single minibatch on  $S = 8$  pipeline stages for varying number of microbatches on 3 different systems: one network bound, one balanced, and one compute-bound.

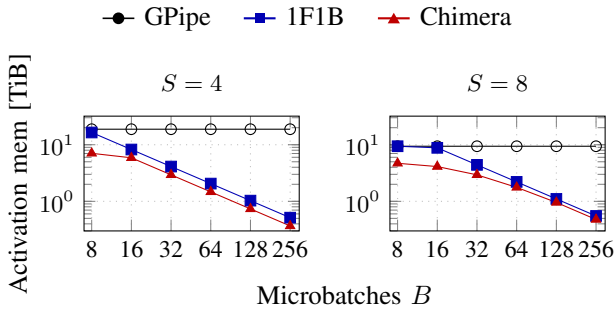


Fig. 5: Peak per-device activation memory consumption for 4 and 8 pipeline stages. Due to its structure GPipe does not change with varying microbatches, since after all forward passes are complete there always is a point in time where the full minibatch of activations resides in memory.

memory consumption is invariant to the microbatch count. Due to its nature to eagerly compute all forward passes, there exists a point in time, after the last forward pass, where the whole minibatch of activations accumulates until they can be deallocated after the respective backward phase. 1F1B reduces the activation-memory peak relative to GPipe by shortening activation-retention intervals once steady state is reached. Chimera lowers activation pressure further in the evaluated settings, but this advantage must be interpreted together with its higher communication demand and possible persistent-memory overheads due to parameter duplication.

#### D. Hanayo in its restricted regime

We additionally compare Chimera against two-wave Hanayo in the restricted  $(S, B) = (8, 8)$  regime, which corresponds to the intended operating point of the schedule. The comparison is summarized in Table I. In this setting, Hanayo outperforms Chimera in eight of the nine modeled systems. Across fast- and medium-network regimes, the runtime improvement is highly consistent, typically in the range of approximately 11%–14%, and is accompanied by noticeably lower idle-time ratios. For

example, on the baseline system, runtime decreases from 59.32s to 51.79s, corresponding to a 12.69% improvement, while idle time drops from 34.51% to 24.99%.

At the same time, this advantage is not robust across all communication regimes. As network performance degrades, the benefit of Hanayo becomes smaller and may disappear entirely. In the `slow_nw_mid_cp` regime, Hanayo improves runtime by only 2.33%, while in the most communication-constrained `slow_nw_fast_cp` regime it becomes 12.32% slower than Chimera and exhibits a higher idle ratio. We therefore interpret Hanayo as effective in its intended restricted operating point, but still sensitive to communication bottlenecks. This result is consistent with the broader conclusion of the paper: even schedules with favorable structural or restricted-regime behavior do not admit a universal ranking independent of the system model.

TABLE I: Comparison of Chimera (C) and two-wave Hanayo (H) in the restricted  $(S, B) = (8, 8)$  regime. Negative  $\Delta T$  means that Hanayo is faster than Chimera.

System	$\beta_{idle}$ [%]		$T_{sim}$ [s]		$\Delta T$ [%]
	C	H	C	H	
fast_nw_fast_cp	35.67	25.47	24.56	21.20	-13.69
fast_nw_mid_cp	34.26	23.76	59.08	50.95	-13.77
fast_nw_slow_cp	33.44	22.79	434.54	374.63	-13.79
mid_nw_fast_cp	36.28	28.31	24.79	22.04	-11.11
baseline	34.51	24.99	59.32	51.79	-12.69
mid_nw_slow_cp	33.47	22.96	434.77	375.47	-13.64
slow_nw_fast_cp	41.73	48.12	27.11	30.45	12.32
slow_nw_mid_cp	36.98	35.47	61.64	60.20	-2.33
slow_nw_slow_cp	33.83	24.65	437.09	383.87	-12.18

#### E. Verdict: schedule rankings are not abstraction-invariant

Taken together, the results across Figures 3, 4, 5, and Table I show that pipeline schedules cannot be ranked reliably from structural reasoning alone. Analytical formulae and instantiated schedule tables may suggest one ordering, but communication-aware simulation can change that ordering once exposed communication, overlap constraints, and system bottlenecks are made explicit.

Under the assumptions considered here, GPipe and 1F1B are runtime-equivalent, but 1F1B achieves a lower memory peak and therefore emerges as the stronger unidirectional baseline. Chimera is advantageous primarily at low microbatch counts and in communication-favorable regimes, where its bidirectional structure can reduce idle time without being dominated by additional communication overhead. Hanayo is effective in its intended restricted regime, but its advantage weakens and can reverse under communication bottlenecks. Overall, no schedule is uniformly superior across abstraction levels and system regimes. The quality of a pipeline schedule is therefore meaningful only in the context of the modeled execution environment.

## VI. CASE STUDY: ASYMMETRIC CHIMERA PLACEMENT

In this section we apply the simulation framework presented in Section III to the Chimera schedule in a what-if analysis. This serves primarily as a demonstration of the applicability of the presented abstractions rather than as a substantial improvement of the existing schedule. Section V-B shows that Chimera, in a low microbatch regime and with sufficient network speeds, offers better run and idle-time ratios and notably lower memory utilization than GPipe and 1F1B. However, as is also the case in 1F1B, the memory pressure is not shared equally across nodes. Typically, the first node in the pipeline has to retain the largest amount of activations, thereby becoming the bottleneck in the overall execution. This begs the question whether this bottleneck can be alleviated through shuffling of intra-pipeline block placement, keeping the total per-device model parameter count fixed.

The original Chimera schedule features two mirrored pipelines over the same device set. In practice, both directions follow the same sequence of stages and distribute blocks uniformly across workers. In theory, nothing disallows a non-uniform distribution. In this experiment we move work from the early stages by assigning fewer blocks to the first half of one of the pipelines and more to the latter half and vice versa for the second pipeline. This maintains a meta symmetry in which each worker still experiences the same amount of work. This split creates some constraints on the model, mainly that the number of blocks be divisible by the number of stages. We thus use  $N = 120$  blocks instead of  $N = 128$ .

Interestingly we do not observe an improvement in global peak memory, only a more uniform distribution across workers. However, we unexpectedly do observe slight improvements in overall runtime. Even more unexpected, there is a strong correlation with the number of stages. The best improvements can be found in shallow pipelines in communication-favorable settings, i.e. fast communication systems. At a depth of  $S = 4$  stages we observe a speedup of 5% compared to the baseline schedule at lower microbatch counts. Going to more stages ( $S = 8$ ), we instead observe a slowdown for few microbatches, but a marginal improvement for larger counts. Figure 6 shows the relative runtime of the unbalanced schedule compared to the baseline balanced schedule.

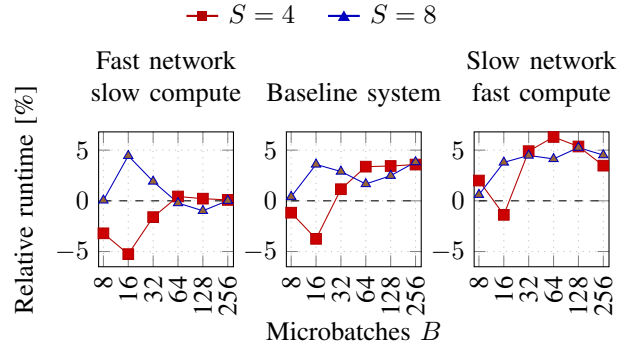


Fig. 6: Relative simulated runtime compared to the baseline Chimera schedule on the network-bound, baseline, and compute-bound system. Lower is better. Interestingly, for 16 microbatches the best and worst results are encountered for the shallow and deeper pipelines respectively.

Although the observed runtime improvements are modest, this case study demonstrates the usefulness of simulation-based what-if analysis. The original goal of reducing peak memory was not achieved, yet the framework still exposed non-obvious runtime behavior that would not have been apparent from either a tabular or purely analytical view.

## VII. CONCLUSION

We introduced a tabular schedule abstraction and a unified multi-abstraction methodology for comparing pipeline schedules in distributed LLM training. By connecting analytical formulae, idealized schedule tables, and communication-aware execution simulation, the framework separates structure-driven from system-driven schedule behavior. Our results show that schedule rankings are not abstraction-invariant: GPipe and 1F1B are runtime-equivalent under the modeled assumptions, but 1F1B has a lower activation-memory peak; Chimera is beneficial mainly at low microbatch counts and in communication-favorable regimes; and Hanayo is effective in its intended restricted regime but remains sensitive to network bottlenecks. The asymmetric Chimera case study further shows that plausible schedule modifications may fail to improve the targeted bottleneck while still revealing non-obvious runtime effects. Overall, pipeline schedule quality cannot be inferred reliably from structural metrics alone, but must be evaluated under an explicit system model that captures communication, dependency, and memory interactions.

For future work, we are particularly interested in extending the framework toward communication-aware energy modeling [15]–[17] and in calibrating the computational model across a broader range of hardware platforms [15], [18]. Another important direction is support for more complex schedule classes, such as interleaved and zero-bubble pipelining [4], [19]. Compression techniques, especially for activation state [20], [21], are also promising, although their evaluation will require modeling quality-efficiency trade-offs.

## REFERENCES

- [1] T. B. Brown, B. Mann, N. Ryder, M. Subbiah, J. Kaplan, P. Dhariwal, A. Neelakantan, P. Shyam, G. Sastry, A. Askell, S. Agarwal, A. Herbert-Voss, G. Krueger, T. Henighan, R. Child, A. Ramesh, D. M. Ziegler, J. Wu, C. Winter, C. Hesse, M. Chen, E. Sigler, M. Litwin, S. Gray, B. Chess, J. Clark, C. Berner, S. McCandlish, A. Radford, I. Sutskever, and D. Amodei, "Language models are few-shot learners," in *Proceedings of the 34th International Conference on Neural Information Processing Systems*, ser. NIPS '20. Red Hook, NY, USA: Curran Associates Inc., 2020. [Online]. Available: <https://dl.acm.org/doi/abs/10.5555/3495724.3495883>
- [2] J. Kaplan, S. McCandlish, T. Henighan, T. B. Brown, B. Chess, R. Child, S. Gray, A. Radford, J. Wu, and D. Amodei, "Scaling laws for neural language models," *CoRR/2001.08361*, 2020. [Online]. Available: <https://arxiv.org/abs/2001.08361>
- [3] M. Shoenybi, M. Patwary, R. Puri, P. LeGresley, J. Casper, and B. Catanzaro, "Megatron-lm: Training multi-billion parameter language models using model parallelism," *CoRR/1909.08053*, 2020. [Online]. Available: <https://arxiv.org/abs/1909.08053>
- [4] D. Narayanan, M. Shoenybi, J. Casper, P. LeGresley, M. Patwary, V. Korthikanti, D. Vainbrand, P. Kashinkunti, J. Bernauer, B. Catanzaro, A. Phanishayee, and M. Zaharia, "Efficient large-scale language model training on gpu clusters using megatron-lm," in *Proceedings of the International Conference for High Performance Computing, Networking, Storage and Analysis*, ser. SC '21. New York, NY, USA: Association for Computing Machinery, 2021. [Online]. Available: <https://doi.org/10.1145/3458817.3476209>
- [5] S. Rajbhandari, J. Rasley, O. Ruwase, and Y. He, "Zero: memory optimizations toward training trillion parameter models," in *Proceedings of the International Conference for High Performance Computing, Networking, Storage and Analysis*, ser. SC '20. IEEE Press, 2020. [Online]. Available: <https://doi.org/10.5555/3433701.3433727>
- [6] Y. Huang, Y. Cheng, A. Bapna, O. Firat, M. X. Chen, D. Chen, H. Lee, J. Ngiam, Q. V. Le, Y. Wu, and Z. Chen, "Gpipe: efficient training of giant neural networks using pipeline parallelism," in *Proceedings of the 33rd International Conference on Neural Information Processing Systems*. Red Hook, NY, USA: Curran Associates Inc., 2019. [Online]. Available: <https://doi.org/10.5555/3454287.3454297>
- [7] D. Narayanan, A. Harlap, A. Phanishayee, V. Seshadri, N. R. Devanur, G. R. Ganger, P. B. Gibbons, and M. Zaharia, "Pipedream: generalized pipeline parallelism for dnn training," in *Proceedings of the 27th ACM Symposium on Operating Systems Principles*, ser. SOSP '19. New York, NY, USA: Association for Computing Machinery, 2019, p. 1–15. [Online]. Available: <https://doi.org/10.1145/3341301.3359646>
- [8] D. Narayanan, A. Phanishayee, K. Shi, X. Chen, and M. Zaharia, "Memory-efficient pipeline-parallel dnn training," in *Proceedings of the 38th International Conference on Machine Learning*, ser. Proceedings of Machine Learning Research, M. Meila and T. Zhang, Eds., vol. 139. PMLR, 18–24 Jul 2021, pp. 7937–7947. [Online]. Available: <https://proceedings.mlr.press/v139/narayanan21a.html>
- [9] S. Li and T. Hoefler, "Chimera: efficiently training large-scale neural networks with bidirectional pipelines," in *Proceedings of the International Conference for High Performance Computing, Networking, Storage and Analysis*, ser. SC '21. New York, NY, USA: Association for Computing Machinery, 2021. [Online]. Available: <https://doi.org/10.1145/3458817.3476145>
- [10] Z. Liu, S. Cheng, H. Zhou, and Y. You, "Hanayo: Harnessing wave-like pipeline parallelism for enhanced large model training efficiency," in *Proceedings of the International Conference for High Performance Computing, Networking, Storage and Analysis*, ser. SC '23. New York, NY, USA: Association for Computing Machinery, 2023. [Online]. Available: <https://doi.org/10.1145/3581784.3607073>
- [11] Z. Jia, M. Zaharia, and A. Aiken, "Beyond data and model parallelism for deep neural networks," in *Proceedings of Machine Learning and Systems*, A. Talwalkar, V. Smith, and M. Zaharia, Eds., vol. 1, 2019, pp. 1–13. [Online]. Available: <https://cs.stanford.edu/~zhiahao/papers/sysml19a.pdf>
- [12] W. Won, T. Heo, S. Rashidi, S. Sridharan, S. Srinivasan, and T. Krishna, "Astra-sim2.0: Modeling hierarchical networks and disaggregated systems for large-model training at scale," in *2023 IEEE International Symposium on Performance Analysis of Systems and Software (ISPASS)*, 2023, pp. 283–294.
- [13] M. Isaev, N. McDonald, L. Dennison, and R. Vuduc, "Calculon: a methodology and tool for high-level co-design of systems and large language models," in *Proceedings of the International Conference for High Performance Computing, Networking, Storage and Analysis*, ser. SC '23. New York, NY, USA: Association for Computing Machinery, 2023. [Online]. Available: <https://doi.org/10.1145/3581784.3607102>
- [14] D. Hendrycks and K. Gimpel, "Gaussian error linear units (gelus)," *CoRR/1606.08415*, 2016. [Online]. Available: <https://arxiv.org/abs/1606.08415>
- [15] L. Braun, S. Nikas, C. Song, V. Heuveline, and H. Fröning, "A simple model for portable and fast prediction of execution time and power consumption of GPU kernels," *ACM Trans. Archit. Code Optim.*, vol. 18, no. 1, pp. 7:1–7:25, 2021. [Online]. Available: <https://doi.org/10.1145/3431731>
- [16] F. Zahn, S. Lammel, and H. Fröning, "On link width scaling for energy-proportional direct interconnection networks," *Concurr. Comput. Pract. Exp.*, vol. 31, no. 2, 2019. [Online]. Available: <https://doi.org/10.1002/cpe.4439>
- [17] J. Tarraga-Moreno, D. Barley, F. J. A. Munoz, J. Escudero-Sahuquillo, H. Froning, P. J. Garcia, F. J. Quiles, and J. Duato, "Scalable and efficient intra- and inter-node interconnection networks for post-exascale supercomputers and data centers," *CoRR*, vol. abs/2511.04677, 2025. [Online]. Available: <https://arxiv.org/abs/2511.04677>
- [18] Y. Emonds, L. Braun, and H. Fröning, "Cudasap: Statically-determined execution statistics as alternative to execution-based profiling," in *23rd IEEE/ACM International Symposium on Cluster, Cloud and Internet Computing*, ser. CCGRID, Y. Simmhan, I. Altintas, A. L. Varbanescu, P. Balaji, A. S. Prasad, and L. Carnevale, Eds. Bangalore, India: IEEE, 2023, pp. 119–130. [Online]. Available: <https://doi.org/10.1109/CCGrid57682.2023.00021>
- [19] P. Qi, X. Wan, G. Huang, and M. Lin, "Zero bubble (almost) pipeline parallelism," in *The Twelfth International Conference on Learning Representations*, 2024. [Online]. Available: <https://openreview.net/forum?id=tuzTN0eIO5>
- [20] D. Barley and H. Fröning, "Compressing the backward pass of large-scale neural architectures by structured activation pruning," *CoRR*, vol. abs/2311.16883, 2023. [Online]. Available: <https://arxiv.org/abs/2311.16883>
- [21] D. Barley and H. Fröning, "Less memory means smaller gpus: Back-propagation with compressed activations," *CoRR*, vol. abs/2409.11902, 2024. [Online]. Available: <https://arxiv.org/abs/2409.11902>